Technical Publication

Coal Pipe Erosion Predictions Using Two Phase Flow CFD

by

Clayton A. Erickson
Staff Engineer
a Babcock Power Inc. company
(formerly DB Riley, Inc.)

Presented at
1998 Joint ASME/JSME
Pressure Vessels and Piping Conference
San Diego, California
July 26-30, 1998

RST-147

Coal Pipe Erosion Predictions Using Two Phase Flow CFD

Clayton A. Erickson, Staff Engineer
DB Riley Inc.
Worcester, MA

ABSTRACT

Multi-burner, pulverized coal-fired boilers have an extensive network of coal pipes which supply the pulverized coal to each individual burner. The balancing of air and coal flows in this network is essential to improving boiler efficiency and reducing boiler emissions. The analysis of coal piping systems is complex due to the two phase nature of the air/pulverized coal mixture and the physical arrangement of the piping system. Due to these complexities, the balancing of coal piping systems using static orifice plates is often difficult. A variable orifice device has been developed which allows on-line balancing of the coal piping system. In a few installations, however, the variable orifice plate has caused excessive coal pipe erosion resulting in operational problems. The variable orifice plate design has been modeled using FLUENT with coal particles accounted for as a discrete second phase. The coal particle trajectories from FLUENT have been post-processed using erosion prediction models to determine relative erosion rates on the pipe surface resulting from the variable orifice plate. The model results indicate that by redesigning the variable orifice blade shape and/or limiting the blade attack angle, the erosion rates can be reduced by an order of magnitude, as compared to the original design.

INTRODUCTION

Pulverized coal fired boilers have coal pipe networks which transport the coal from the pulverizers to the individual burners using air as the conveying medium. Figure 1 shows a typical coal pipe arrangement for an electric utility boiler with three pulverizers and twelve burners. Utility boilers can have as many as 16 pulverizers feeding 112 individual burners. The geometric location and number of pulverizers and burners create a complex coal pipe network with different coal pipe lengths, bends and elevations. These complex system arrangements create unbalanced system flow resistances among the coal pipes. These system imbalances cause an uneven distribution of coal and primary air between the burners, which results in a wide range of burner zone stoichiometries and combustion zone temperatures. The production of nitrogen oxides (NO_X) and the efficiency of the carbon burnout in the furnace are both dependent upon balanced burner zone stoichiometries and combustion zone temperatures [Lisauskas et al. 1989, Penterson et al. 1993]. Therefore, the balancing of the coal and primary air in the coal pipe network is essential for the control of NO_X emissions and for efficient carbon burnout.

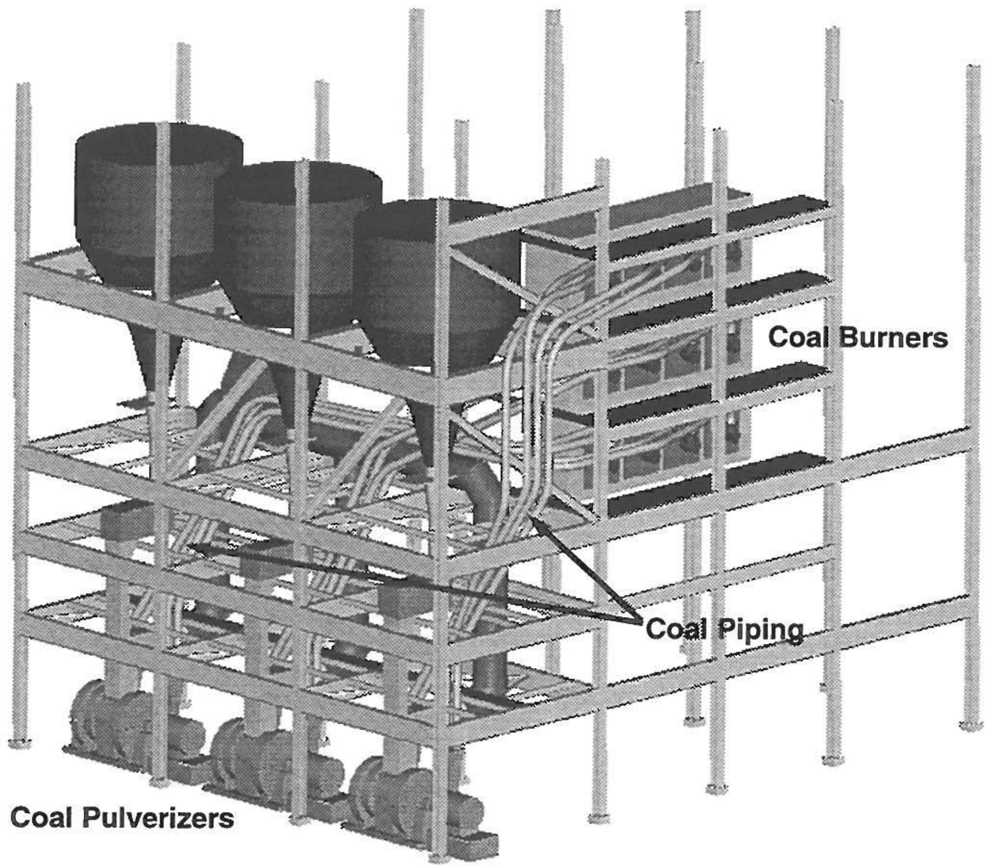

Figure 1 Typical Coal Pipe Arrangement

One method to balance the air/coal flow in the coal piping network is to place fixed orifice plates of varying sizes into the coal piping based on a two phase pressure drop calculation procedure accounting for both air pressure losses and coal particle pressure losses. This method accounts for unbalances resulting from geometric differences among the pipes but not for dynamic imbalances caused by varying resistances in pulverizers and burners. One or more primary air fans supply the air to the pulverizers and each pulverizer can have a different resistance due to varying internal wear, different classifier settings, etc. In order to account for the dynamic imbalances caused by the pulverizers, the air flow in each coal pipe is measured during boiler operation with both air and pulverized coal flowing in the pipe. The balancing of the coal pipe network requires that the pressure drop in each coal pipe be adjusted based on the flow measurements taken during boiler operation. If fixed orifices were used, each pulverizer system (and possibly the boiler) would have to be taken off-line for the installation of the orifices. This would be a time consuming and expensive operation. A variable orifice plate, Figure 2, has been developed which allows the on-line adjustment of the pressure drop in any coal pipe. With the variable orifice plate the coal pipe network can be adjusted dynamically to account for varying system resistances.

The balancing of coal pipe networks with the variable orifice plate shown in Figure 2 has proved very successful. However, accelerated coal pipe erosion at some installations resulted in unacceptable coal wear rates. The rate of wear is dependent upon the abrasive characteristics of the coal, orifice blade shape and the attack angle of the variable orifice plate as discussed herein. A new blade shape, shown in Figure 3, was designed to replace the existing blade shape. This paper reports on a CFD analysis of the potential of the new blade shape to reduce coal pipe erosion as compared to the original blade shape.

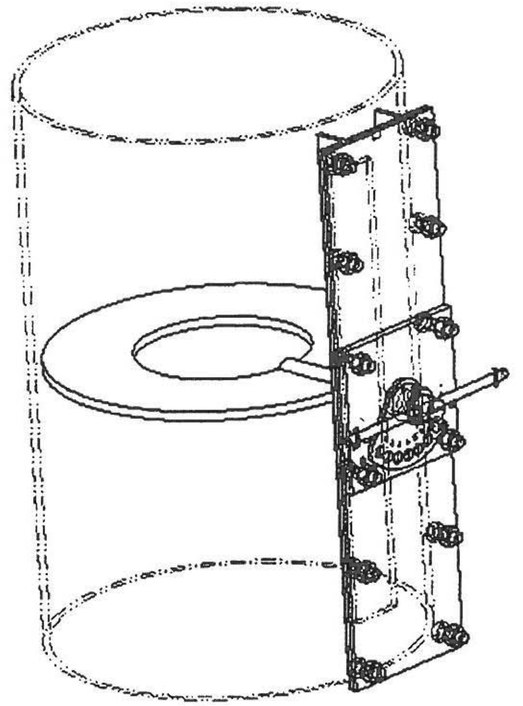

Figure 2 Variable Orifice Plate, Original Design (U.S. Patent 5,593,131)

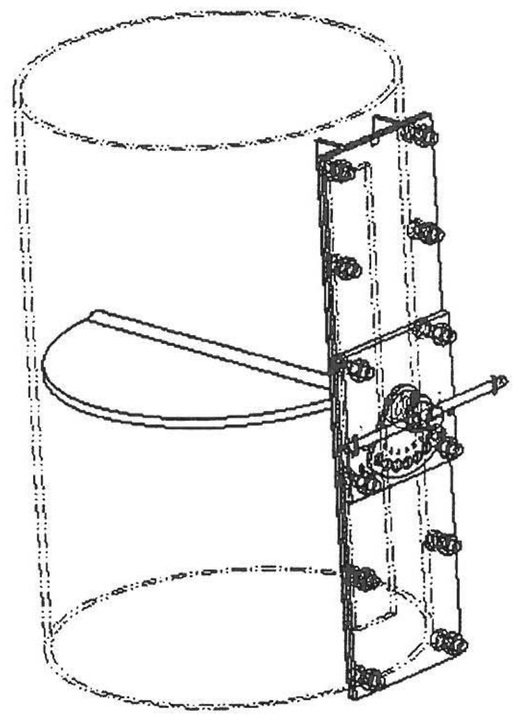

Figure 3 Variable Orifice Plate, New Design (Patent Pending)

THE COMPUTATIONAL MODEL

Geometry

The two dimensional model geometry studied is an upward flowing vertical coal pipe of 13.25 inch inner diameter with 7 pipe diameters upstream and 15 pipe diameters downstream, see Figure 4. The blade attack angle is measured relative to the x-axis with a 0° attack angle being perpendicular to the flow. Two variable orifice blade configurations are studied, the original design and the new design. The effect of blade attack angle to the flow is investigated by studying both 30° and 45° blade attack angles for both blade designs.

CFD Solution

A steady state FLUENT/UNS model using the Standard k-e turbulence model is used to solve the fluid flow problem. The model geometry was meshed using triangular elements. The number of elements was adjusted during the solution phase using FLUENT's mesh adaptation features and the total number of elements varied between 8,000 to 80,000 depending on the blade type and angle. The inlet air boundary condition has a uniform velocity distribution. The fluid flow model was an air phase only model using constant fluid properties. Table 1 gives the fluid conditions used for this model, which are typical conditions for pulverized coal piping. The pulverized coal particles were not coupled to the solution of the fluid flow problem in order to reduce computational effort. The coal particle trajectories are determined by injecting the particles into the converged fluid flow field.

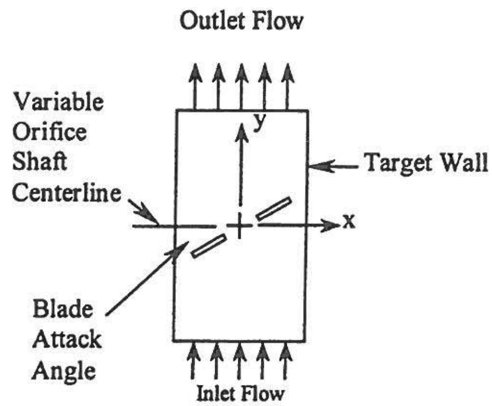

Figure 4 Computational Model Geometry

Table 1 Computational Model Fluid Properties

Temperature, °F (°C)	150 (65.5)
Pressure, iwc (mbar)	10 (24.86)
Inlet Velocity, ft/sec (m/sec)	74.0 (22.5)
Density, lbm/ft^3 (kg/m^3)	0.061. (0.977)
Viscosity, lbm/ft sec (cP)	1.363×10^{-5} (2.03×10^{-2})

Erosion Model

The erosion model utilized closely follows the works of Hutchings [1974, 1979], Walsh, Beer and Sarofim [1987] and Bauver et al. [1984]. The dimensionless relative erosion is calculated using the following functional form:

$$E = KMf(\theta)V^n$$

Where:

E is the dimensionless erosion rate

K is the particle/target material erosion proportionality constant

V is the impacting particle velocity

M is the impacting particle weight

$f(\theta)$ is the impact efficiency of the impacting particles

n is the velocity power coefficient

The impact efficiency of the particles is only a function of the impact angle of the particle shown in Figure 5. The value of K is set to one, and all erosion rates are normalized to the largest erosion rate calculated. This normalization procedure allows comparison of the relative erosion rates between blade designs and attack angles without specific knowledge of coal particle erosion characteristics. The value of the velocity power coefficient is set to 2.25 following the work of Bauver et al. [1984].

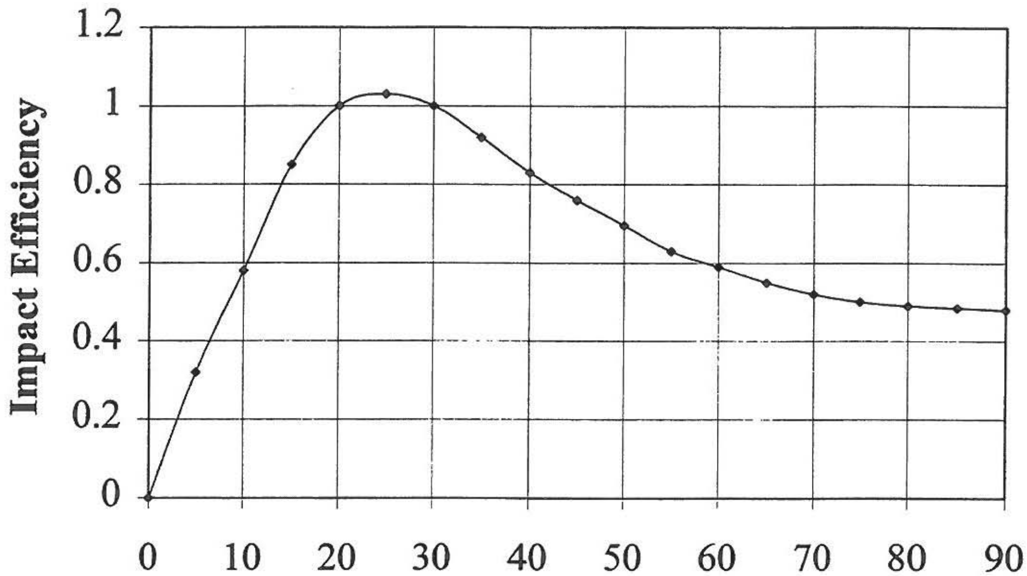

Figure 5 Impact Efficiency vs. Impact Angle

Coal Particle Injections

The coal particle size distribution was governed by a Rosin-Rammler distribution with typical pulverized coal values. Nine coal particle sizes where injected as listed with mass and volume percentages in Table 2.

Table 2 Injected Coal Particle Properties

Particle Size, (Microns)	Particle Diameter, (ft)	Percent of Particles, Mass Basis	Percent of Particles, Volume Basis
30	9.84×10^{-5}	45	91.3
50	1.64×10^{-4}	14	6.1
70	2.29×10^{-4}	10	1.6
90	2.95×10^{-4}	8	0.6
100	3.28×10^{-4}	3	0.16
150	4.92×10^{-4}	9	0.14
200	6.56×10^{-4}	5	0.083
250	8.20×10^{-4}	2.5	8.76×10^{-3}
290	9.51×10^{-4}	3.5	7.86×10^{-3}

The coal particles are introduced uniformly along the inlet of the coal pipe with an initial velocity of 70 ft/sec. down the pipe. A uniform number of each of the nine particle sizes of either 500 or 1000 particles were injected for each statistical sample. The number of particles injected varied based on available disk space on the workstation, a typical output file size for a 1000 particle injection is 700 MB.

The coefficient of restitution for a coal particle collision with a steel target is not well known. For collisions between both lead and glass with steel, the coefficient of restitution is reported to be 0.30 and 0.60 respectively. Based on this data, a coefficient of restitution of 0.45 was used in these calculations to compare the varying blade designs and attack angle settings. The sensitivity of the relative erosion to the coefficient of restitution was studied by varying the coefficient from 0.30 to 0.60 for the case of the original blade design at an attack angle of 30°.

The trajectory of the coal particles is determined using a stepwise integration over discrete time steps in a stochastic random walk method. The instantaneous value of the fluctuating fluid flow velocity, due to turbulence, is predicted using a random number generator. The resulting positional and velocity data for each particle at each time step from the stepwise integration is written by FLUENT to an ASCII output file. If the coal particle strikes the target wall the particle is trapped, the data for the collisions are recorded and the integration stops for that particle. The output data file is post-processed using a FORTRAN program that calculates the relative erosion rate for particles that collide with the target wall, using the functional form of the dimensionless relative error. Each statistical sample releases a uniform number of all particle sizes; therefore to adjust the erosion calculations for the desired particle distribution, the percent of particles on a volume basis is used as a weighting factor. The target wall is divided into 0.5 inch bins starting at the variable orifice shaft centerline and extending 30 inches down stream. The weighted relative erosion of the coal particles that collide with the target is summed for each bin.

To account for the statistical variations in the turbulent flow, multiple coal particle sample injections are performed. The number of statistical sample injections required is determined by measuring the error in the relative erosion rate for each 0.5 inch bin using the equation.

$$error = \frac{\left| \sum_{n=1}^{N-1} E - \sum_{n=1}^{N} E \right|}{\sum_{n=1}^{N-1} E} \times 100$$

Where:

N is the total number of statistical samples

E is the dimensionless relative erosion rate

Depending on the number of particles injected per sample, the relative erosion rate converged to within a maximum of 1% for any 0.5 inch bin with 30 to 50 statistical samples.

Results and Discussion

The fluid flow field solutions for the two blade designs and various attack angles were converged to a maximum residual of 0.0001 for all equations. The original blade design with an attack angle of 45° required the greatest number of cells, approximately 80,000 due to the stability of the vortices behind the blade.

The trajectories of the coal particles of the smallest and largest diameters with the original blade design at an attack angle of 30° are shown in Figures 6 and 7 respectively. The smallest particles, 30 Micron, illustrate the effect the fluid flow field has on the particles; all the particles that collide with the upstream blade segment are entrained in the flow without striking the wall, while many of the particles that strike the down stream blade segment are directed into the target wall. Conversely, the largest particles, 290 Microns, striking either blade segment collide with the target wall as indicated in Figure 7. This difference in behavior shows that the relative erosion rate is a function of the coal particle size distribution. In the current work the coal particle size distribution is fixed to simulate typical operating conditions.

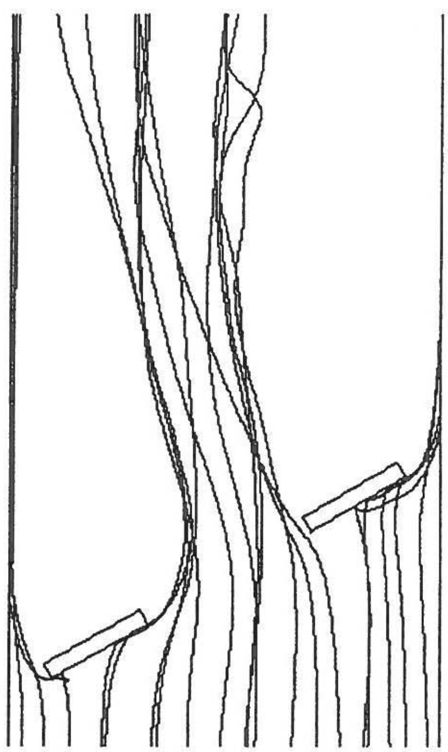

Figure 6 Coal Particle Trajectories. Coal particle diameter of 30 Micron, original blade design, attack angle 30°, 20 particles injected.

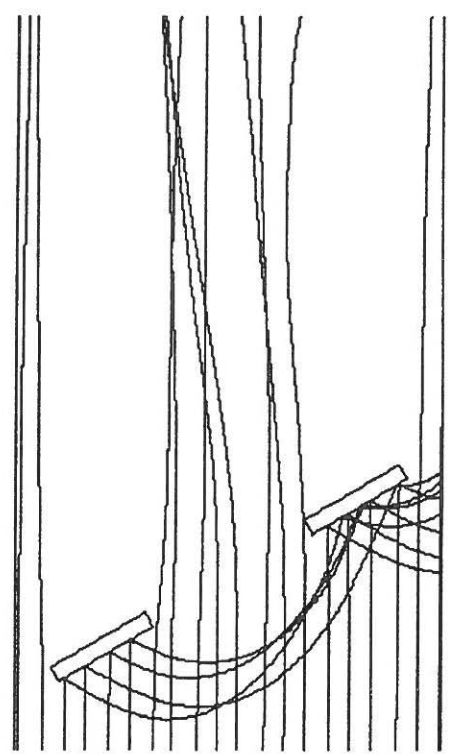

Figure 7 Coal Particle Trajectories. Coal particle diameter of 290 Microns, original blade design, attack angle 30°, 20 particles injected.

The trajectories of the coal particles of the smallest and largest diameters with the new blade design at an attack angle of 30° are shown in Figures 8 and 9 respectively. The smallest particles, 30 Microns, show the effect the blade design has on the air flow patterns and therefore the particle trajectories. In contrast to the original design, few of the particles collide with the wall as a result of striking the blade. However similar, to the original design, the largest particles, diameter 9.51×10^{-4}, striking the blade segment collide with the target wall. Due to the small percentage of large particles in the pulverized coal flow, this continued collision event does not result in adverse erosion rates.

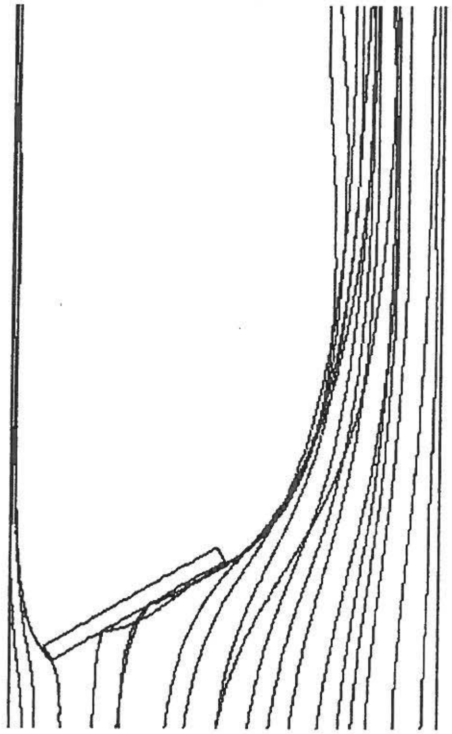

Figure 8 Coal Particle Trajectories. Coal particle diameter of 30 microns, new blade design, attack angle 30°, 20 particles injected

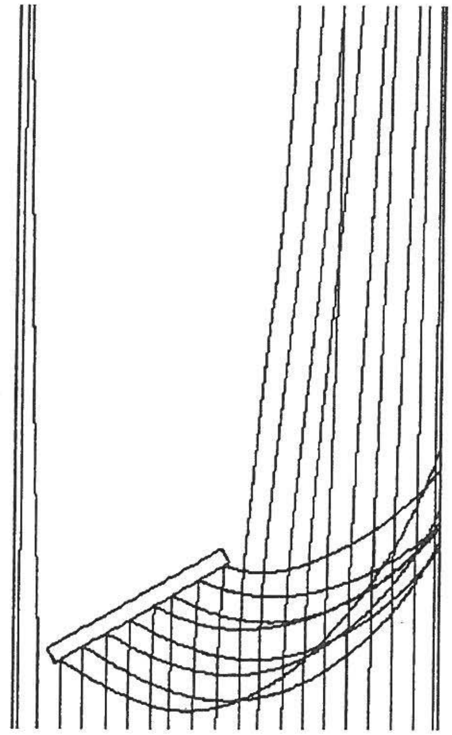

Figure 9 Coal Particle Trajectories. Coal Particle diameter of 290 Microns, new blade design, attack angle 30°, 20 particles injected.

The relative erosion vs. distance from the shaft centerline for the original blade design with attack angles of 30° and 45° is shown in Figure 10. This figure illustrates the effect the blade attack angle has on the relative erosion. The relative erosion rate is reduced by 70%, for the original blade design, by changing the blade attack angle from 30° to 45°. The blade attack angle of 30° also concentrates the relative erosion over a small area. The location of the highest relative erosion for the 30° attack angle case matches well with operating unit data. The relative erosion is normalized based on the maximum erosion rate for the original blade design with an attack angle 30°.

The effect of the coefficient of restitution on the relative erosion vs. distance from the shaft centerline is shown in Figure 11. The figure indicates that, for the current problem conditions, the magnitude and location of the relative erosion is a weak function of the coefficient of restitution.

The effect of blade design on relative erosion for attack angles of 30° and 45° are shown in Figures 12 and 13 respectively. Both figures show that the original blade design creates small regions of high erosion rates. The figures further indicate that the new blade design reduces the relative erosion by an order of magnitude for a given angle of attack. Comparing the relative erosion for the original blade design with a 30° angle of attack to that of the new blade design with a 45° angle of attack shows a reduction in erosion rates by 40 times. The blade attack angle changes the maximum relative erosion rate by a factor of 3 and 4 for the original and new blade design respectively.

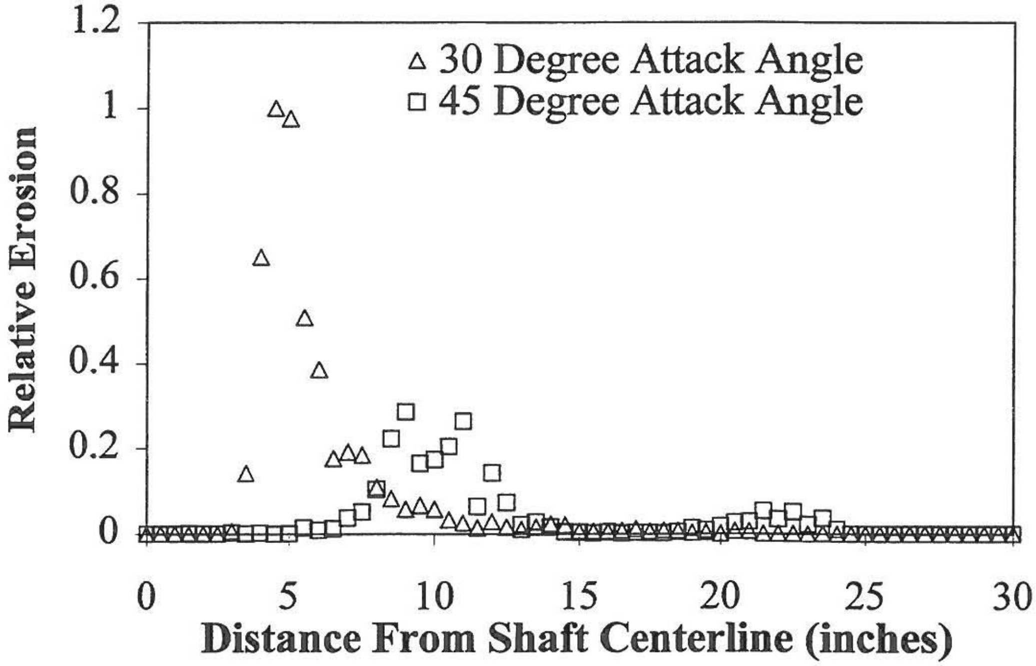

Figure 10 Relative Erosion vs. Distance from Shaft Centerline as a Function of Blade Attack Angle. Original blade design with a coefficient of restitution of 0.45

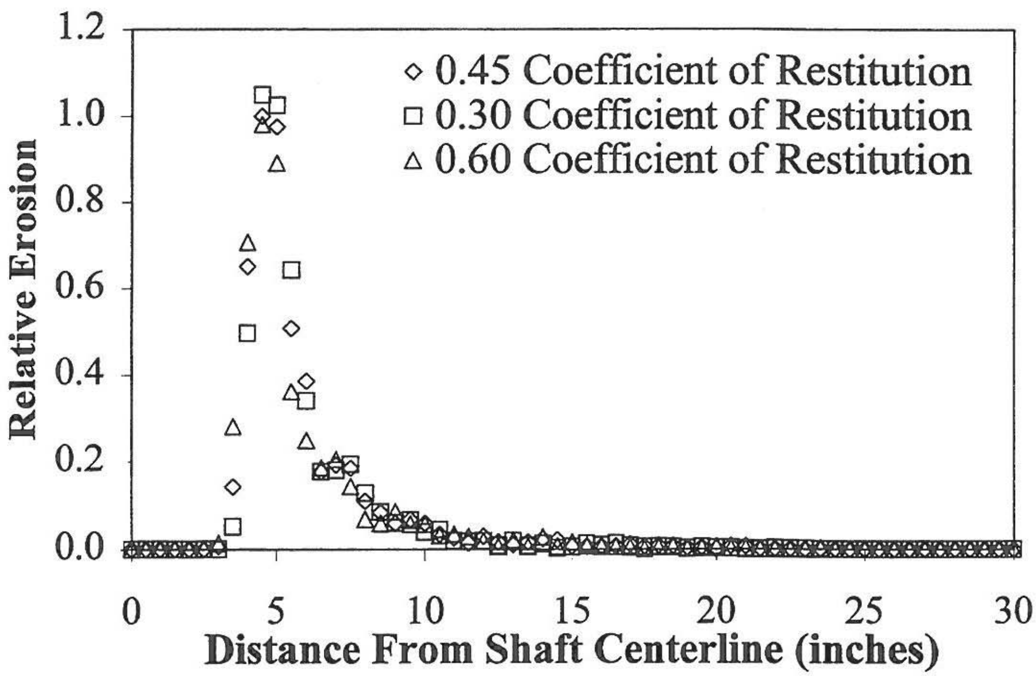

Figure 11 Relative Erosion vs. Distance from Shaft Centerline as a Function of Coefficient of Restitution. Original blade design with an attack angle of 30°

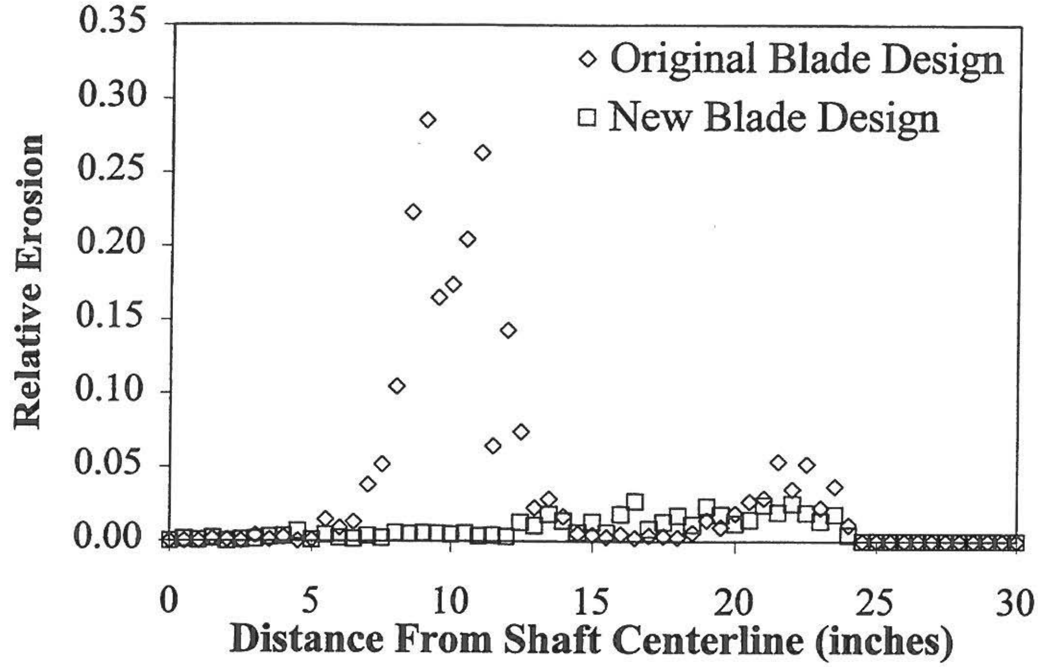

Figure 12 Relative Erosion vs. Distance from Shaft Centerline as a Function of Blade Design with an Attack Angle of 30°

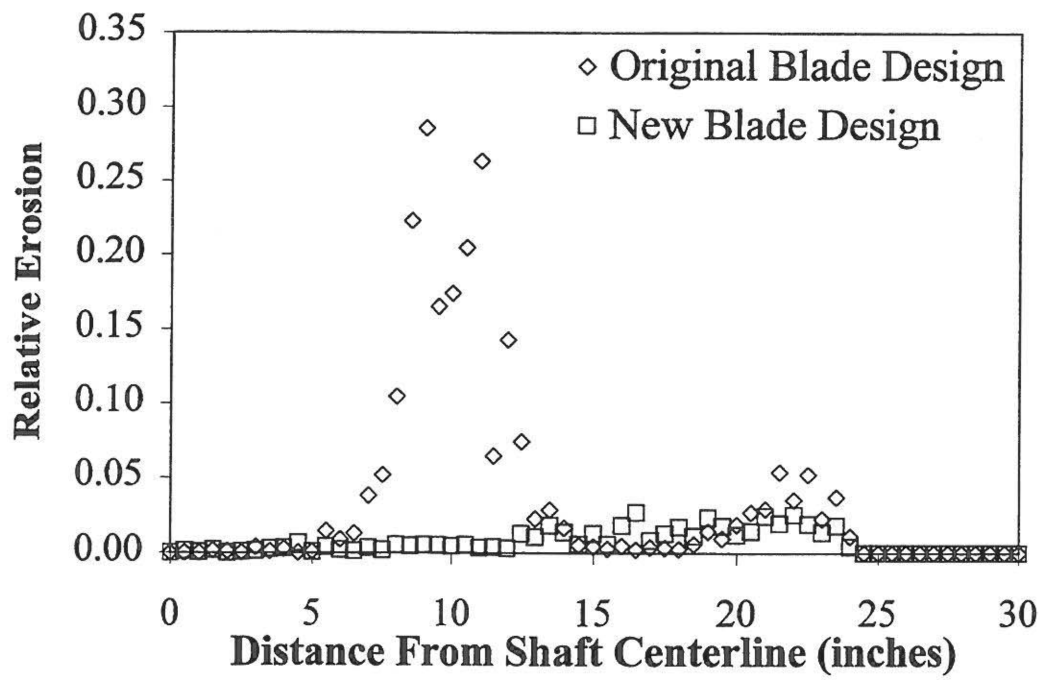

Figure 13 Relative Erosion vs. Distance from Shaft Centerline as a Function of Blade Design with an Attack Angle of 45°

CONCLUSIONS

The new blade design of the variable orifice plate can reduce the relative erosion rate by an order of magnitude with both a 30° and 45° angle of attack. The relative erosion rate is shown to be a weaker function of the blade attack angle for the new design as compared to the original design. The location and magnitude of the relative erosion rates are a weak function of the coefficient of restitution.

REFERENCES

Bauver, W.P., Bianca, J.D., Fishburn, J.D. and McGowan, J.G., 1984, "Characterization of Erosion of Heat Transfer Tubes in Coal Fired Power Plants," ASME Paper Number 84-JPGC-FO-3, New York.

Hutchings, I. M., 1974, "The Erosion of Ductile Metals by Solid Particles," Ph.D. Dissertation, University of Cambridge, Cambridge.

Hutchings, I. M., 1979, "Mechanisms of the Erosion of Metals by Solid Particles," in A.S.T.M. STP 664, "Erosion: Prevention and Useful Application".

Lisauskas, R. A., Reicker, E. L., Davis, T., 1989, Status of NOx Control Technology at Riley Stoker," 1989 Joint Symposium on Stationary Combustion NOx Control, San Francisco.

Penterson, C. A., Lisauskas. R. A., 1993, "Applications and Further Enhancement of the Low NOx CCV Burner," EPRI/EPA NOx Symposium, Miami Beach.